



UNIVERSITÀ DEGLI STUDI DI NAPOLI
FEDERICO II

Dottorato di Ricerca in

“ORGANISMI MODELLO NELLA RICERCA BIOMEDICA E
VETERINARIA”

**A SPONTANEOUS MOUSE MODEL OF
X-LINKED MYOPATHY WITH
EXCESSIVE AUTOPHAGY**

Relatore:

Ch.mo Prof.

Orlando Paciello

Candidata:

Dott.ssa

Valentina Iovane

XXIV Ciclo

INTRODUCTION	4
1.1. Autophagic Vacuolar Myopathies.....	4
<i>Acid maltase deficiency (Pompe disease)</i>	7
<i>Danon disease</i>	9
<i>Infantile autophagic vacuolar myopathy (AVM-I)</i>	10
<i>Childhood autophagic vacuolar myopathy with sarcolemmal features (C-AVM-SF)</i>	10
<i>Autophagic vacuolar myopathy with multiorgan involvement (AVM-Mo)</i>	11
<i>Autophagic vacuolar myopathy with dilated cardiomyopathy</i>	11
1.2. Differential diagnosis of AVMs	12
2. Autophagy	13
2.1. <i>Autophagy - a housekeeping process</i>	14
2.2. <i>Autophagy – the lysosomal component</i>	17
2.3. <i>Autophagy in skeletal muscle</i>	20
3. X-LINKED VACUOLAR MYOPATHY WITH EXCESSIVE AUTOPHAGY ...	21
3.1. <i>Clinical presentation</i>	22
3.2. <i>Epidemiology</i>	23
3.3 <i>Electromyography</i>	23
3.4 <i>Genetics</i>	24
3.5. <i>V-ATPase pump</i>	27
3.6 <i>Features of C57 mouse</i>	32
EXPERIMENTAL PART	35
4. Materials and Methods	35
4.1 <i>Light microscopy</i>	35
4.2 <i>Immunohistochemistry</i>	36
4.3 <i>Electron microscopy</i>	37
4.4 <i>Immunoblot</i>	37

4.5 Genetics	38
5.Result.....	39
5.1 Light microscopy	39
5.2 Immunohistochemistry.....	41
5.3 Electron microscopy	43
5.4 Immunoblot	44
6. Discussion	47
7 .References	52

LIST OF ABBREVIATIONS

AVM: Autophagic Vacuolar Myopathy

AVM-I: Infantile Autophagic Vacuolar Myopathy

AVM-SF: Autophagic Vacuolar Myopathy with Sarcolemmal Features

AVSF: Autophagic Vacuoles with Sarcolemmal Features

EM: Electron microscopy

EMG: Electromyography

LAMP: Lysosomal-Associated Membrane Protein

MAC: Membrane-Attack Complex of the Complement

MHC: Major Histocompatibility Complex

V-ATPase: Vacuolar ATP-ase

XMEA: X-linked Myopathy with Excessive Autophagy

INTRODUCTION

A myopathy is a muscular disease in which the muscle fibers do not function resulting in muscular weakness. "Myopathy" simply means muscle disease (myo- Greek μυο "muscle" + pathos -pathy Greek "suffering").

There are two class of myopathy: congenital and acquired. Among congenital myopathy, particularly, there is a class of metabolic myopathy caused by a difect in lysosomal function, these are called "Lysosomal Storage Disease". Lysosomal storage diseases are a group of more than 45 genetically determined heterogenous metabolic disorders.

The majority are characterized by deficient activity of specific lysosomal hydrolases and the intralysosomal accumulation of one or more substrates in affected cells.

These vacuolar myopathies are defined by the presence within myofibers of circumscribed spaces called vacuoles. Vacuolar pathology is one of the most common pathologies in skeletal muscle disease.

1.1. Autophagic Vacuolar Myopathies

Autophagic Vacuolar Myopathies (AVMs) are an emerging group of conditions characterized by presence in the sarcoplasm of large, membrane-bound true vacuoles (not artifacts of tissue preparation) filled with partially degraded cellular components including proteins, glycogen, and degenerating organelles (1).

The presence of varied cytoplasmic constituents in partially degraded state

within the vacuoles led to terming these vacuoles, and the diseases, “Autophagic”.

Currently there are different AVMs (Table 1).

Table 1. Autophagic vacuolar myopathies

DISEASE NAME	REFERENCE
Danon Disease	Danon MJ et al.(1981)
Pompe Disease	Pompe JC(1932)
X-linked myopathy with excessive autophagy	Kalimo H et al.(1988)
Infantile autophagic vacuolar myopathy	Yamamoto A et al.(2001)
Childhood autophagic vacuolar myopathy	Yan C et al.(2005)
Autophagic vacuolar myopathy with multiorgan involvement	Kaneda D et al.(2003)
Autophagic vacuolar myopathy with dilated cardiomyopathy	Sugimoto S et al.(2007)

The origin of the vacuolar membrane in AVMs is unknown.

A subgroup of AVMs is characterized by vacuoles possessing sarcolemmal features (AVSF). Sarcolemma is the plasma membrane of the myofiber and is surrounded by the extracellular matrix, called basement membrane, with two layers: the basal lamina, in direct contact with the sarcolemma, and the outer reticular lamina (fig.1).

The membrane of vacuoles with sarcolemmal features displays proteins that are otherwise localized to the intracellular face of sarcolemma and on the basal lamina, such as, but not restricted to, dystrophin and laminin $\alpha 2$. Of the AVSFs, the most frequent are Danon disease and X-linked myopathy with excessive autophagy (XMEA), the latter representing the focus of this thesis.

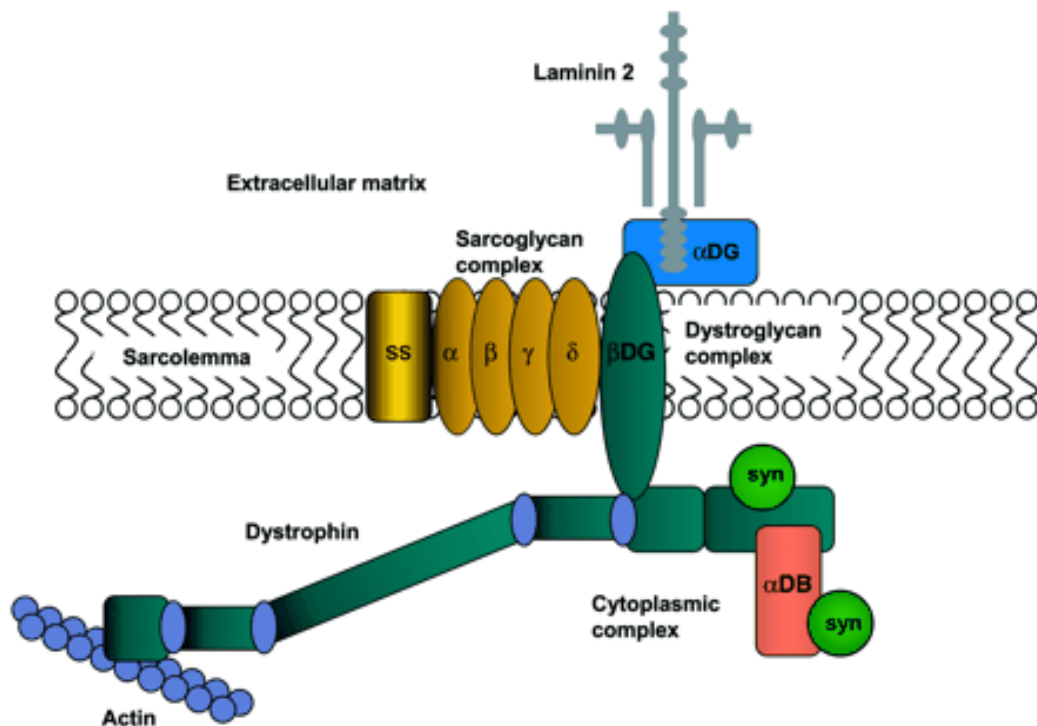


Fig.1: Sarcolemma and basement membrane-associated proteins

The dystrophin-associated protein complex (DPC) in skeletal muscle. Dystrophin binds to cytoskeletal actin at its NH₂ terminus. At its COOH terminus, dystrophin is associated with a number of integral and peripheral membrane proteins that can be classified as the dystroglycan subcomplex, the sarcoglycan-sarcospan subcomplex, and the cytoplasmic subcomplex. The cytoplasmic subcomplex includes the syntrophins (syn) and -dystrobrevin (DB). The sarcoglycan-sarcospan subcomplex comprises the sarcoglycans and sarcospan. The extracellular component of the dystroglycan complex, -dystroglycan (DG), binds to laminin-2 in the extracellular matrix and -dystroglycan (DG) in the sarcolemma. In turn, -dystroglycan binds to the dystrophin, thus completing the link between the actin-based cytoskeleton and the extracellular matrix.

Acid maltase deficiency (Pompe disease)

Pompe disease (glycogen storage disease type II) is an autosomal recessive disorder which damages muscle and nerve cells throughout the body. It is caused by an accumulation of glycogen in the lysosome due to deficiency of the lysosomal acid maltase, an enzyme which catalyzes the hydrolysis of α -1,4 and α -1,6 links of glycogen. As a result, glycogen accumulates inside lysosomes, primarily in cardiac and skeletal muscle (fig.2). Complete acid maltase deficiency causes a rapidly progressing disease in infants, who die of cardiac failure before age 2. Partial deficits lead to late-onset forms, when cardiac muscle is usually spared and the phenotype is dominated by a slowly progressive myopathy with respiratory insufficiency. Microscopic examination of muscle biopsy shows variable-sized vacuoles that are strongly positive for the lysosomal acid phosphatase, indicative of lysosomes, predominantly in type I fibers. Although in some late-onset forms the vacuolar membrane may react with markers of dystrophin, this feature is not constant and does not include many sarcolemmal and basal lamina proteins. There is diffuse increase in glycogen staining in muscle and acid maltase activity is reduced or absent. Recent results show that in Pompe disease, all the vesicles of the endocytic/autophagic pathways rather than just lysosomes are dramatically expanded and less mobile, while a subset of late endosomes/lysosomes have increased pH. These findings suggest that Pompe lysosomes, apart from lacking acid maltase, also have a defect in fusing with and cause hydrolases to autophagic vacuoles (2).

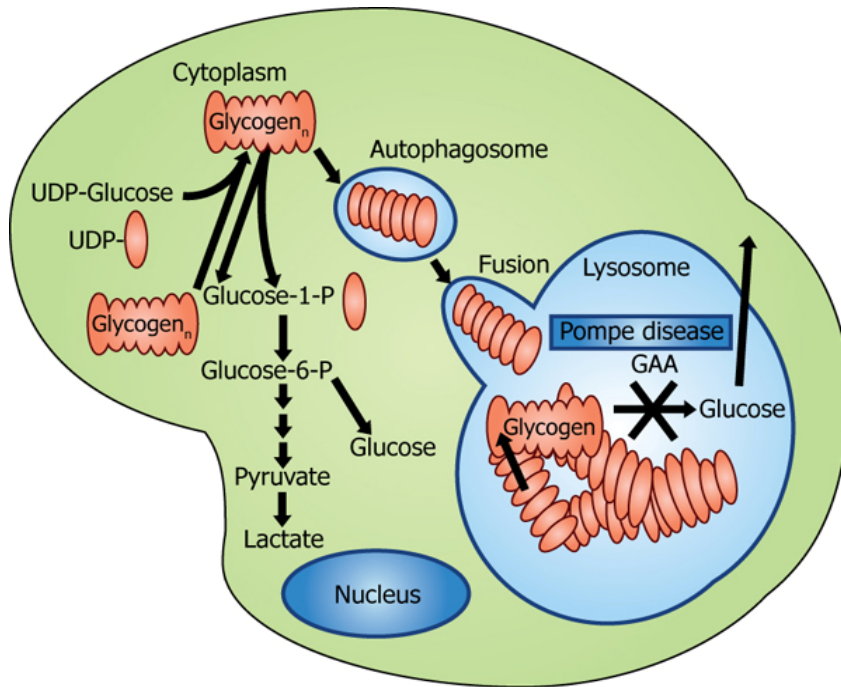


Fig.2: Pompe disease pathway

Glycogen builds up in cells and is taken up by the lysosomes.

In Pompe disease, it cannot be broken down into glucose and therefore accumulates in the lysosomes, causing tissue damage.

Danon disease

Danon disease was the first AVM-SF described by Moris Danon in 1981.

The phenotype is characterized by the triad cardiomyopathy, myopathy and mental retardation.

Inheritance is X-linked, with males being affected predominantly, while carrier mothers usually have milder and later-onset cardiac symptoms. Muscle biopsy is diagnostic and shows vacuoles containing cellular debris, including cytoplasmic degradation products and glycogen.

The vacuolar membrane is positive for dystrophin and delineated by basal lamina.

Nishino et al. (3) showed that Danon disease is caused by inactivating mutations in the *LAMP2B* isoform of the *LAMP2* gene (lysosomal-associated membrane protein) on chromosome Xq24, encoding a lysosomal membrane protein (3). In the absence of *LAMP2B*, lysosomes appear unable to merge with and provide enzymes to autophagic vacuoles (4). As a result, autophagosome maturation is impaired and they accumulate in the cytosol (5). A LAMP2-deficient mouse has been created that proved a valuable model of Danon disease. These mice show extensive accumulation of autophagic vacuoles in many tissues including liver, pancreas, spleen and kidney, beside heart and skeletal muscle (6).

Infantile autophagic vacuolar myopathy (AVM-I)

Two vacuolar myopathy patients with unusually severe phenotype and early onset were reported by Yamamoto et al. (7). Both patients were hypotonic at birth, presented with cardiomegaly and died in early infancy. Acid maltase and LAMP-2 staining were positive in heart, skeletal muscle and liver that contain glycogen granules.

Pathological examination showed a picture similar to XMEA because these the two diseases are allelic.

Childhood autophagic vacuolar myopathy with sarcolemmal features (C-AVM-SF)

In 2005, Yan et al. (8) reported a large family with a different phenotype than known AVMSFs.

The family included seven affected male members of Chinese-American background. Of these, five died during infancy. The surviving two members were hypotonic infants and developed cardiomyopathy, dyspnea and dysphagia. Serum creatine kinase levels were elevated. Muscle pathology revealed autophagic vacuoles with sarcolemmal features, multilayered basal lamina with marked sarcolemmal deposition of C5-b9 membrane attack complex and calcium, histologically indistinguishable from childhood-onset X-linked myopathy with excessive autophagy (XMEA).

No female relatives, including the carriers, were affected. Haplotype analysis suggests that this new AVM and XMEA may be allelic despite different clinical presentations.

Autophagic vacuolar myopathy with multiorgan involvement (AVM-Mo)

Kaneda et al. (9) reported a 41-year-old man with a novel form of adult-onset autophagic vacuolar myopathy (AVM) with multiple organ involvement including eyes, heart, liver, lung, kidney, and skeletal muscle. Serum creatine kinase was slightly elevated. The vacuolar membranes had sarcolemmal features similar to vacuoles in Danon disease, X-linked myopathy with excessive autophagy, and infantile AVM.

Lysosome associated membrane protein-2, absent in Danon disease, was present. Vacuolation was also present in heart and liver. Defined by distinct clinical features, this disease constitutes the fourth entity in the group of autophagic vacuolar myopathy in which the vacuolar membranes have features of sarcolemma.

The disease-causing gene in congenital AVM is not known at the present time.

Autophagic vacuolar myopathy with dilated cardiomyopathy

Recently, a late-onset case of AVM with cardiomyopathy of the dilated type was reported by Sugimoto et al. (10). The patient, of Japanese background, came from a family with history of consanguineous marriage. Unlike previously-described late-onset AVM, other organs beside muscle were unaffected. Serum creatine kinase was ~ 10 times above normal values. Acid maltase activity of the muscle was normal, but the biopsied muscle specimen stained for lysosome-associated membrane protein-2 (LAMP-2), which has been reported to be deficient in muscles of patients with Danon disease. The clinical features of the patient are distinct from X-linked myopathy with excessive autophagy, infantile autophagic vacuolar myopathy and autophagic vacuolar myopathy with late-onset and multiorgan involvement.

The gene defect responsible is not known.

1.2. Differential diagnosis of AVMs

AVM entities can be separated from one another based on clinical and pathological criteria (Table 2)

Table 2. Differential diagnosis of AVMs

	Pompe disease	Danon disease	XMEA	Infantile AVM	Childhood AVM	AVM with multiorgan involvement	AVM with dilatated cardiomyopathy
Myopathy onset	Infancy and adulthood	Teenage years	6-18 years	infancy	Early childhood	adulthood	adulthood
Myopathy severity	Respiratory muscles involved	mild	mild	Early death	Early death in same cases	mild	mild
Cardiomiopathy	+	+	-	+	+/-	+	+
Mental retardation	-	+	-	NA	-	-	-
Other organs involved	-	+	-	NA	-	+	-
LAMP2 protein	+	-	+	+	+	+	+
Acid maltase	-	+	+	+	+	+	+
Vacuoles with sarcolemmal features	-	+	+	+	+	+	+
Basement membrane duplication	-	-	+	+	+	-	NA

2. Autophagy

The term “autophagy”, coming from the Greek words for “eating oneself”, refers to any process of degradation of intracellular components by lysosomes.

Three types of autophagy (fig.3) have been described to date:

- In *chaperone-mediated autophagy*, the lysosome takes in proteins to be digested via specific receptors
- *Microautophagy* happens when lysosomes directly engulf cytoplasm by invaginating, protrusion, and/or septation of the lysosomal limiting membrane.
- *Macroautophagy* is responsible for the bulk degradation of long-lived proteins and aged organelles .

Macroautophagy sequesters damaged organelles and unused long-lived proteins in a double-membrane vesicle, called an autophagosome or autophagic vacuole (AV), inside the cell. Autophagosomes form from the elongation of small membrane structures known as autophagosome precursors. Increased macroautophagy means increased formation of autolysosomes, but in XMEA each new autolysosome undergoes a degradative block and is slow to progress and disappear. Increased formation coupled with delayed progression results in vast numbers of autolysosomes, in some cells fusing together and forming giant autophagic vacuoles and autophagic vacuolation identical to the disease in muscle that gives XMEA its name, “excessive autophagy” (11).

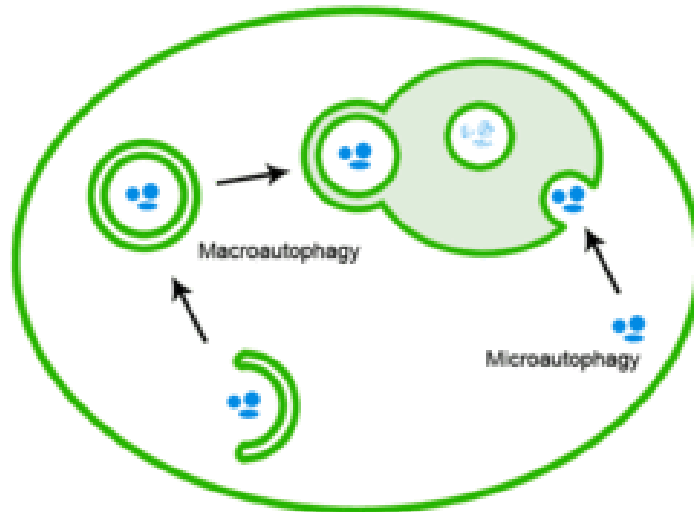


Fig.3: Macro and Microautophagy

In microautophagy, organelles and/or cytosolic proteins are engulfed by the vacuolar membrane and degraded in the vacuole lumen. Macroautophagy involves the formation of large (300-900 nm) cytosolic, double-membrane vesicles (autophagosomes), which sequester organelles and/or cytosolic proteins. Once formed, autophagosomes fuse with the vacuole, releasing a single-membrane vesicle (autophagic body) into the lumen of this organelle where the autophagic bodies are degraded

2.1. Autophagy - a housekeeping process

Autophagy have different functions: nutrient starvation, infection, repair mechanism and programmed cell death.

Autophagy was initially described as a particular adaptation response of the cell to starvation: when external nutrients become limited, the cell continues to maintain energy production and macromolecular synthesis by digesting and re-utilizing old or non-essential cellular components.

Autophagy plays a role in the destruction of some bacteria within the cell.

Intracellular pathogens such as *Mycobacterium tuberculosis* persist within cells and block the normal actions taken by the cell to rid itself of it. Stimulating autophagy in infected cells overcomes the block and helps to rid the cell of pathogens.

Autophagy degrades damaged organelles, cell membranes and proteins, and the failure of autophagy is thought to be one of the main reasons for the accumulation of cell damage and aging.

Autophagy occurs with formation of a transient organelle called “autophagosome”, a double-membrane vacuole that delivers the components to be destroyed to the lysosome.

The origin of the autophagosomal membrane is controversial; it arises as a membrane sac (*phagophore*) that expands around a cytosol portion containing the target. The autophagosomes merge with lysosomes and become autolysosomes, which possess lysosomal pH and acid hydrolases (12). Lysosomal enzymes rapidly degrade the vacuolar content along with the inner membrane layer and the autolysosome is cleared from the cytosol (fig. 4). The process ends up when the remaining lysosome releases for recycling, through lysosomal membrane permeases, macromolecules resulted from digestion. As basal autophagy takes place at a low rate, microscopic observation of autophagic vacuoles in healthy tissues is a rare instance. Regulation of autophagy is extremely complex and involves pathways overlapping with control of cell growth, proliferation, cell survival and death.

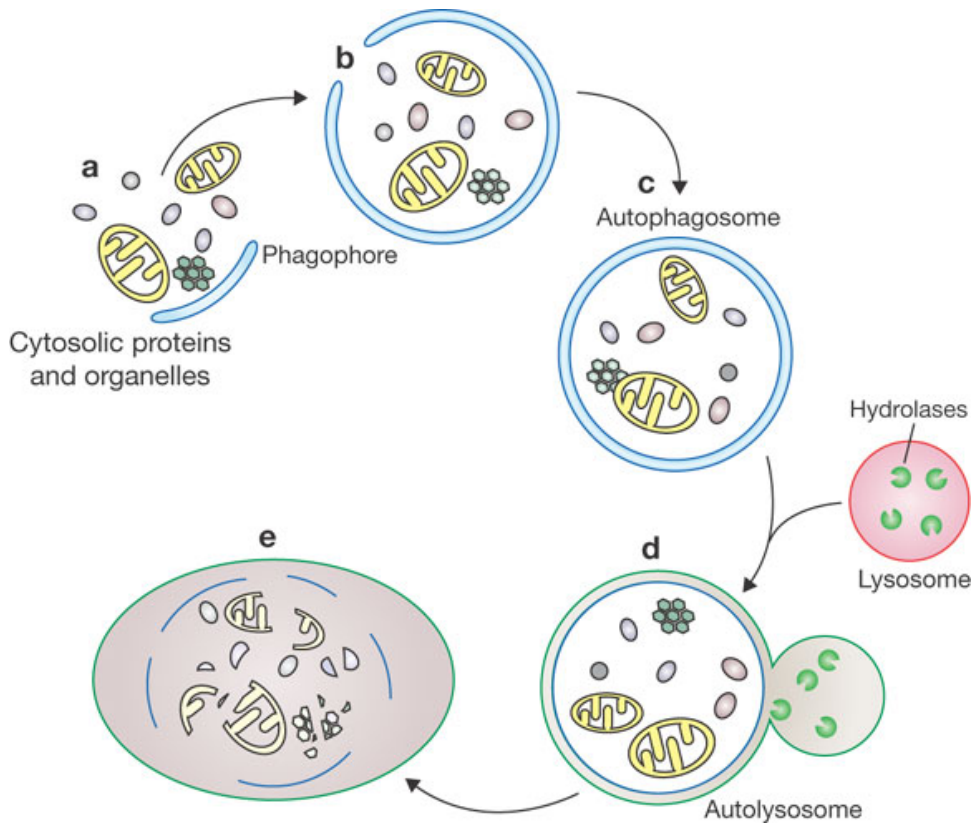


Fig.4:Autophagosome formation and clearance

(a, b) Cytosolic material is sequestered by an expanding membrane sac, the phagophore;

(c) resulting in the formation of a double-membrane vesicle, an autophagosome;

(d) the outer membrane of the autophagosome subsequently fuses with a lysosome, exposing the inner single membrane of the autophagosome to lysosomal hydrolases;

(e) the cargo-containing membrane compartment is then lysed, and the contents are degraded.

2.2. Autophagy – the lysosomal component

The lysosome is the primary disposal and recycling apparatus of the cell. It degrades cellular and extracellular macromolecules, providing aminoacids, fatty acids, nucleic acids, and carbohydrate residues for reutilization in cellular synthesis. DeDuve coined the term *lysosome* in Greek meaning “litic body”, in 1955 to describe a sedimentable acidified cytoplasmic organelle containing various hydrolases that degrade cellular and extracellular products and foreign materials ingested by the cell(fig.5).

The lysosomal membrane protects the cell from the destructive action of the degradative enzyme within it (6).

To begin the process of intracellular digestion, a hydrolase-free vacuoles containing macromolecular material coalesces, via the lysosomal associated protein-2 (LAMP-2). The vacuoles contain intracellular debris (autophagy) or extracellular foreign (eterophagy).

Following digestion of the macromolecules, their individual components are transported to the cytosol for reutilization. These dense polymorphic bodies are able to leave the cell to be taken up by other cells and for the extracellular digestion of connective tissue and bone. Lysosomal enzymes are glycoproteins that act on lipids, carbohydrates, proteins, and nucleotides to catalyze irreversibly their hydrolysis to their basic structural units. The genes coding for many of these enzymes have been mapped to specific human chromosomes. Lysosomes contain up to 50 types of acid hydrolases, including proteases, nucleases, glycosidases, lipases, phospholipases, phosphatases and sulphatases. These enzymes are synthesized in the endoplasmic reticulum (ER) and a hydrophobic aminoterminal signal peptide on the nascent protein directs its transport

into the lumen of the RER, where it undergoes glycosylation of selected asparagines residues. Maturation of lysosomal enzymes is a three-step process depending on successively lower pH: mannose 6-phosphorylation in the Golgi (pH 6.5), removal of mannose in endosomes (pH 5.5) that transport the enzymes to the lysosome, and finally cleavage of preproteins into shorter active forms in the lysosome (pH 4.7).

Lysosomal pH is critical for optimal activity of acid hydrolases. It is mainly controlled by an ATP-consuming complex, the vacuolar ATP-ase (V-ATPase).

The lysosomal protein in a vesicular form then enters the Golgi apparatus where a series of covalent modifications occur to the transported proteins. The pathway and targeting signal for lysosomal membrane proteins differs from those used by soluble lysosomal hydrolases. The two best-know lysosomal-associated membrane proteins (LAMP) are LAMP-1 and LAMP-2. These two glycoproteins are structurally similar and evolutionarily related. Expression of LAMP-2 is increased in tissues of mice deficient in LAMP-1. LAMP-2 is a family of membrane proteins, and LAMP-2a was identified as a receptors in lysosomes known as chaperone-mediated autophagy. Recent studies indicate that LAMP-2 may be involved in the process of fusion of autophagic vacuoles with lysosomes.

Lysosomal disorders are triggered when a particular enzyme exists in a small amount or is entirely missing. When this happens, substances accumulate in the cell.

In other words, when the lysosome doesn't function normally, excess products destined for breakdown and recycling are stored in the cell. Clinically, the initial manifestations begin in childhood and, in many of these disorders, death can occur at an early age. In many, the central nervous system is particularly affected, because neurons whose function is impaired by lysosomal storage lack the ability to regenerate.

Nearly all lysosomal storage diseases are inborn errors of metabolism. The

majority are inherited as autosomal recessive traits. For many of the diseases, severe infantile, less severe juvenile, and milder chronic or late-onset forms are known.

Such individuals are totally deficient in the relevant enzyme activity and usually have a severe clinical form of the disease. Muscle cells in patients with lysosomal diseases tend to shrink because of central nervous system degeneration, with resulting denervation.

There is loss of contractile elements and exocytosis of their lysosomal content. Thus, standard light microscopy of muscle is not very useful for the diagnosis of the majority of lysosomal storage diseases because of relative size, amount, and solubility of the storage material.

Most of these disorders are autosomal recessively inherited however a few are X-linked recessively inherited (6).

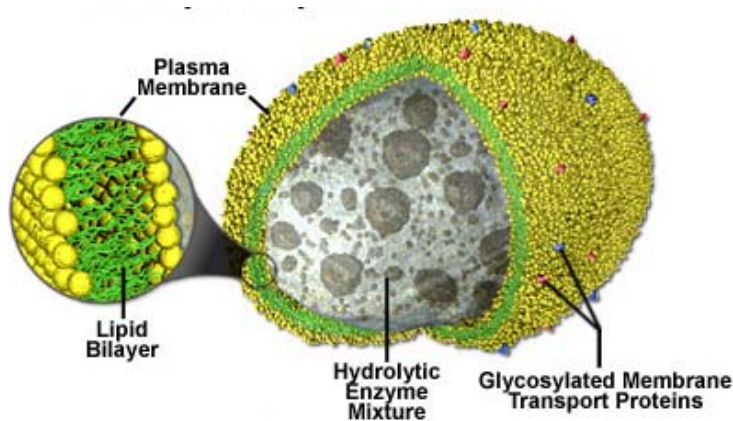


Fig.5: Anatomy of the Lysosome

lysosomes are spherical organelles contained by a single layer membrane, though their size and shape varies to some extent. This membrane protects the rest of the cell from the harsh digestive enzymes contained in the lysosomes, which would otherwise cause significant damage. The cell is further safeguarded from exposure to the biochemical catalysts present in lysosomes by their dependency on an acidic environment.

2.3. Autophagy in skeletal muscle

The lysosomal system in normal skeletal muscle is poorly developed. One possible reason is that muscle does not normally engage in absorptive, secretory, or excretory activities. Normal skeletal muscle contains a full complement of acid hydrolases. There are two populations of lysosomes in skeletal muscle. Those from the muscle itself account for 75 to 95 percent of the enzyme activity. Lysosomal enzyme activities are higher in fetal muscle and muscle of young animals than in muscle of older animals. Histochemical studies demonstrate greater activity in the oxidative than in the glycolytic fibers (6).

As discussed above, the autophagic process depends on regulated ATG genes and, at the other end, on lysosomes being able to fulfil their clearance function. Tissue vacuolation has been linked to either massive up-regulation of autophagy that overcomes lysosomal capacity of clearance, and/or to defective lysosomes that fail to clear even steady-state autophagosomes, although evidence of step-to-step processes leading to vacuolation is missing.

However, not every tissue is equally prone to vacuolation. Vacuolar myopathies are the most common muscle diseases, suggesting that muscle is particularly susceptible to deregulation of the autophagic process. This is further supported by the fact that muscle is preferentially affected in diseases caused by lysosomal defects, although the defect exists throughout the organism (like Danon disease and Pompe disease). Recent data confirm and help explain particularities of autophagy in muscle.

Bechet et al. (13) reported that of all tissues, skeletal muscle has the fewest lysosomes. At the same time however, as shown by Mizushima et al. (2004), skeletal muscle has the highest macroautophagic activity after stimulation (14).

Interestingly, although stimulation of autophagy in muscle elicits an ample response in terms of autophasome numbers, the size of these is small, even smaller than autophagosomes in other tissues and very small compared to the giant autophagic vacuoles that characterize XMEA pathology (14).

3. X-LINKED VACUOLAR MYOPATHY WITH EXCESSIVE AUTOPHAGY

In 1988, Kalimo et al. (15), described a new type of X-linked myopathy in a Finnish family. The clinical course was characterized by slow progression of muscle weakness without loss of ambulation in childhood and no evidence of cardiac, respiratory, or central nervous system involvement. Muscle fibers were not necrotic and showed excessive autophagic activity and exocytosis of the phagocytosed material.

These authors proposed the name X-linked myopathy with excessive autophagy (XMEA) (15).

3.1. Clinical presentation

XMEA usually begins in childhood, progresses slowly, and affects skeletal muscle exclusively. Patients have normal life expectancy. All affected patients are male. Obligate female carriers either are asymptomatic or manifest subtle clinical, electromyographic, or muscle biopsy findings. Typically, the onset is between ages 6 and 18 years with weakness and gradual wasting of the proximal muscles of the lower extremities. The affected boy achieves all the normal motor milestones, followed by gradual inability to keep up with his companions in running and climbing.

Other skeletal muscle groups are progressively affected including the upper limb girdle and distal muscles. The typical clinical feature is slowly progressive proximal weakness, most marked in the lower limbs. Muscle fibers are not necrotic and show excessive autophagic activity and exocytosis of the phagocytosed material. Significant muscle wasting, most marked in the quadriceps, occur in adults. Cardiac muscle involvement is notably absent. Patients may become wheelchair-bound in their fifties, but lifespan is generally not affected. However, in some cases, life expectancy was shortened due to respiratory muscle involvement (6).

The central and peripheral nervous system, heart and other organs are clinically unaffected. Generally, plasma levels of serum creatine kinase are considered proportional to the degree of muscle cell destruction by necrosis. The moderate increase in serum creatine kinase in XMEA however is not explained by the total lack of necrosis. Kalimo et. al suggested that it may arise by extrusion of creatine kinase molecules together with other exocytosed material once vacuoles fuse with the sarcolemma and open to the extracellular space (15).

3.2. Epidemiology

XMEA is rare and probably under-diagnosed. To date, few families have been reported and the ethnic backgrounds were different: Finnish, French, American, English, Kurdish, Armenian and Italian. The actual disease prevalence will become clear in the coming years with the availability of genetic testing.

3.3 Electromyography

EMG consists in recording of the electrical activity of muscle by inserting a needle electrode in the muscular mass. Recordings are made while muscle is at rest, as well as during passive and active contractions. Various neuromuscular disorders determine specific electrical response patterns. A nerve conduction velocity test is usually performed at the same time, when small electrical shocks are applied to measure the ability of the nerve to conduct electrical signals.

In XMEA patients, nerve conduction studies are normal. EMG examination reveals myopathic changes, including striking myotonic and high-frequency discharges in all muscles, even clinically unaffected facial, bulbar and distal limb muscles (16).

Myotonia represents a state of hyperexcitability of muscle fibers in which a voluntary contraction or electromechanical stimulation can provoke trains of repetitive action potentials and causes a delay in relaxation after muscle contraction. It is a feature in human disorders caused by dysfunctions of ion channels in the muscle membrane.

Interestingly however, the EMG aspect of myotonia in XMEA patients is not accompanied by clinical myotonia. This rare situation of EMG-without-clinical myotonia was only described in rare cases of myotonic dystrophy type 2, adult-onset acid maltase

deficiency myopathy, myositis and thyroid myopathy (19), all clinically different from XMEA.

In conclusion, EMG in XMEA is characteristic and can be used in conjunction with pathologic examination as a tool to distinguish XMEA from other myopathies and AVMs.

3.4 Genetics

The first reported XMEA family (1988) originated from Finland. A four-generation pedigree was assembled that showed 5 affected males and no affected females; the disease was carried on from generation II to generation IV through a female who had affected sons from two marriages. This pedigree strongly suggested an X-linked mode of inheritance (15). Myopathies known to be linked to the X chromosome at the time were Duchenne-Becker muscular dystrophy at Xq21, Emery-Dreifuss muscular dystrophy in the distal part of Xq and Danon disease that was thought to be a more severe form of XMEA. Although clinical presentation was different in XMEA, the possibility of novel mutations with effect on other functional domains or only affecting particular tissue isoforms of these genes could not be excluded.

In 1988, Saviranta et al. (17) attempted a linkage study in the original Finnish family. They analyzed segregation of restriction fragment length polymorphisms belonging to 17 loci across the X chromosome in III-2 and her sons (4 informative meioses). Based on these genotyping results, the authors further calculated logarithm of odds (LOD) scores for linkage between each of the loci and XMEA gene at different

recombination fractions. The most likely linkage for XMEA was obtained with marker DXS15 on the most distal chromosomal band, Xq28. This excluded allelism with Duchenne-Becker muscular dystrophy. However, the LOD score based on this only XMEA family at the time was too low to establish with certitude linkage to Xq28.

In 2000, two separate studies firmly confirmed that XMEA gene was indeed linked to Xq28. Villard et al. (18) used the reported French XMEA family to construct an exclusion map of the X chromosome by analyzing segregation of 32 polymorphic markers distributed evenly across the chromosome. The entire chromosome except Xq28 was excluded so the candidate gene may be located in chromosome Xq28. The gene appears to be close to the Emery-Dreifuss gene so they also sequenced the emerin gene, responsible for Emery-Dreifuss muscular dystrophy, in three patients from three different XMEA families, without finding mutations. These results excluded allelism between XMEA and Emery-Dreifuss muscular dystrophy .

They also sequenced two candidate genes: the bigly-can gene, BGN, which encodes a protein that links the sarcoglycan complex to the basal lamina, and the gene for filamin A, which anchors the plasma membrane to the extracellular matrix. Other sequenced candidate genes in the region are emerin, and LAMP-2 mutated in Danon disease (6). In parallel, Auranen et al. (18) genotyped members of a Danon disease family for markers spanning the entire X chromosome. Haplotype analysis of two affected brothers excluded the region telomeric to marker DXS8091 as carrying the disease gene, thus showing that XMEA and Danon are not allelic (the possibility that a very large gene that would span to the region outside Xq28 was considered and excluded based on genome analysis). Together, results from these two studies placed the XMEA gene in a region telomeric to marker DXS1193, spanning 10.5 cM.

Minassian et al. (18) collected seven new families in the following two years and

genotyped the family members for known and newly described markers across the 10.5 cM XMEA region. Three families have proved informative: two French families with an identical haplotype in affected members telomeric to marker DXS10053 and an American family where a recombination event resulted in identical haplotypes in two affected brothers only telomeric to the same marker DXS10053. These observations allowed narrowing of the disease locus to a 4.37 Mb region telomeric to marker DXS10053.

Genetic analysis selected different candidates genes for XMEA in particular Ramachandran et al.(11) focuses their attention on LOC203547 . LOC203547 encodes for a 101 amino acid protein which is named VMA21.

The LOC203547 has three exons and a 4.7 Kb tran script expressed in all tissues.

The mutations consist of six different single-nucleotide substitutions.

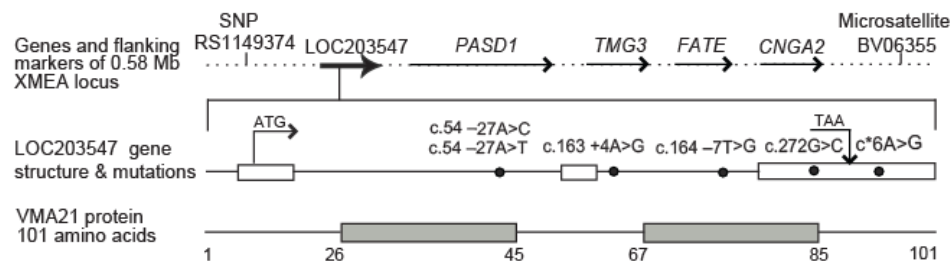


FIG.6:identification of XMEA gene

*The first two, c.54 -27A/T and c.54 -27A/C, eliminate the A nucleotide predicted to define the first intron's splice branch point. The third, c.163 +4A/G, removes the A in the +4 position after exon 2 that is required for optimal U1 small nuclear RNA (snRNA) binding during splicing. The fourth, c.164 -7T/G, disrupts the polypyrimidine tract in intron 2, which would reduce the U2AF splice factor binding efficiency. A fifth, c.272G/C, is in coding sequence replacing a glycine with alanine, but it also abolishes a predicted splice enhancer site. The sixth, c.*6A/G, is in the 30 untranslated region (UTR).*

3.5. V-ATPase pump

Ramachandran et al. in 2009 (11), show that XMEA is caused by hypomorphic alleles of the VMA21 gene, that VMA21 is the diverged human ortholog of the yeast Vma21p protein, and that like Vma21p it is an essential assembly chaperone of the V-ATPase, the principal mammalian proton pump complex. The V-ATPase is a multi-subunit enzymatic complex that accomplishes against-gradient transfer of [H⁺] ions across membranes using energy resulted by breakdown of ATP.

V-ATPases acidify lysosomes and regulate the pH of multiple systems in the cell, including the secretory pathway and the endovesicular system, which use gradated pH to accomplish stepwise modifications.

The V-ATPases (fig.7) are ubiquitous in endomembrane systems of all cells, and in humans and other species are also expressed at the plasma membrane of specialized cells that secrete acid (11).

The V-ATPase complex is composed of 14-to-date protein subunits, organized into a transmembrane domain (V0) and a peripheral domain (V1)(19). The a subunit of the V0 sector spans the membrane and forms within it two separate channels that are not continuous one with the other. One channel starts in the cytoplasm and ends within the membrane lipid bilayer, and the other starts from a different location in the lipid bilayer and opens in the organelle lumen. Protons enter from the cytoplasm into the first channel and exit within the bilayer. There, they load onto the side of a cylinder (composed of V0 subunits c, c', c'' and d) which rotates and transports them to the entrance of the second a channel, through which they exit into the organelle. The torque that rotates this cylinder is provided by the V1 complex, which generates the force by consuming ATP.

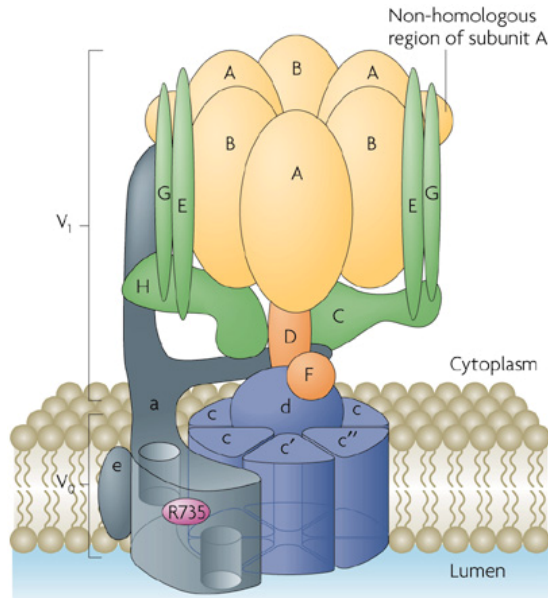


FIG.7: V-ATPase pump

The vacuolar (V-)ATPase complex is composed of a peripheral domain (V1, shown in yellow and orange), which is responsible for ATP hydrolysis, and an integral domain (V0, shown in blue and grey), which is involved in proton translocation across the membrane¹. The core of the V1 domain is composed of a hexameric arrangement of alternating A and B subunits, which participate in ATP binding and hydrolysis. The V0 domain includes a ring of proteolipid subunits (c, c' and c'') that are adjacent to subunits a and e. The V1 and V0 domains are connected by a central stalk, composed of subunits D and F of V1 and subunit d of V0, and multiple peripheral stalks, composed of subunits C, E, G, H and the N-terminal domain of subunit a. Subunit a possesses two hemi-channels and a crucial buried Arg residue (R735), which are required for proton translocation across the membrane. The depiction of the N-terminal domain of subunit a having two lobes comes from the observation that this domain interacts with subunits C and H near the membrane interface^{24, 102} and with the non-homologous region of subunit A⁶⁹, which appears from electron microscopy images to be located about two-thirds of the way up the outer surface of V1. It is likely that in the isolated V0 domain¹³ the N-terminal domain of subunit a can interact with rotor subunits (such as subunit d) in the free V0 complex, which therefore prevents rotation and passive proton translocation through free V0.

V-ATPases are also expressed in the plasma membranes of specialized cells and contribute to multiple functions, such as renal acidification, bone resorption, sperm maturation, and control of cytoplasmic pH.

Mutations in cell-specific isoforms of V-ATPase subunits cause tissue-specific diseases.

V-ATPase function caused by mutations in an essential chaperone, VMA21, that result in muscle-specific disease in humans (20).

The Ramachandran et al.(11) show that VMA21 deficiency decreases V-ATPase activity, resulting in an increase in intralysosomal pH. This increase in pH impairs lysosomal action and blocks the autophagic degradation of proteins leading to accumulation of autophagosomes and autophagic vacuoles.

Ramachandran et al. further postulate that the block in autophagy would result in upregulation of macroautophagy.

In agreement with this notion, they did observe an increase in early components of the macroautophagic activation pathway including beclin-1, beclin-1-hVps34 complexes, and LC3. They further propose that decreased recycling of excess and degraded proteins and the reduced liberation of amino acids enhances autophagy because a decrease in amino acids in the cytoplasm modulates the mTOR signaling pathway, which then upregulates macroautophagy (Fig. 8).

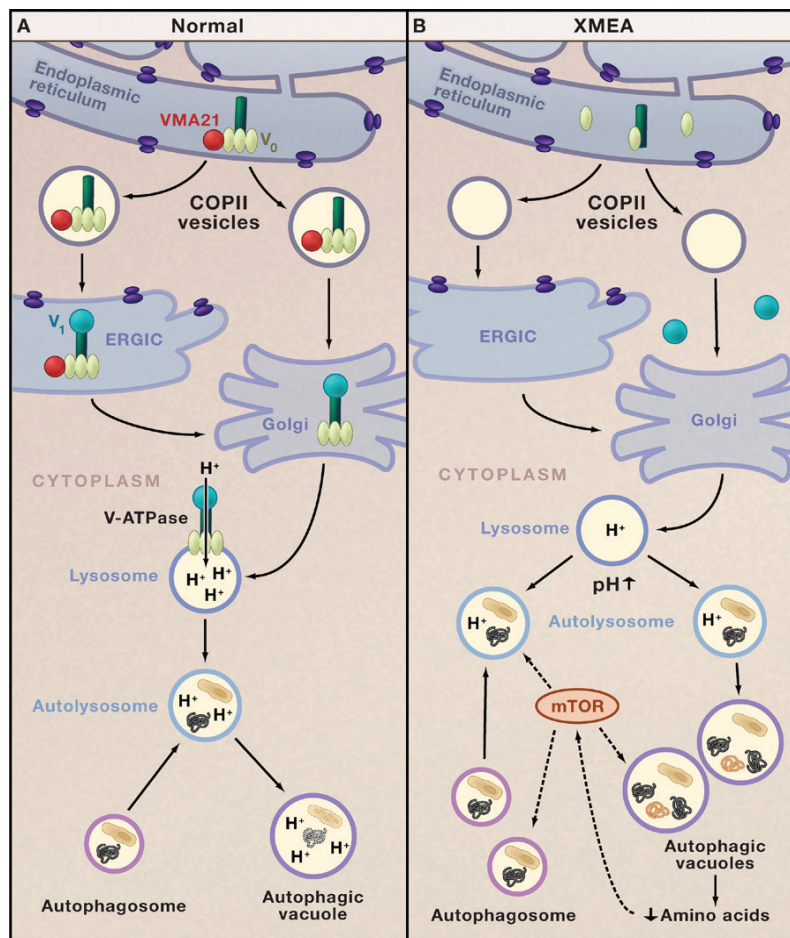


Fig.8: V-ATPase and Autophagy in Health and Disease

(A) The chaperone VMA21 (red circle) binds to the c'' subunit of the vacuolar-ATPase (V-ATPase; dark green) in the endoplasmic reticulum and initiates assembly of the proton-translocator domain (V0; pale green). VMA21 chaperones V0 in COPII vesicles to the endoplasmic reticulum Golgi intermediate complex (ERGIC). VMA21 is not present in the Golgi apparatus, but it is here that V-ATPase assembly is completed by addition of the ATP-hydrolytic domain (V1; turquoise). Proton pumping by the V-ATPase is critical for regulating the pH of lysosomes. Fusion of lysosomes with autophagosomes generates autolysosomes that degrade target proteins and organelles.

(B) In the disease X-linked myopathy with excessive autophagy (XMEA), deficiency of VMA21 leads to failure of V0 assembly, reduced levels of V-ATPase, and a decrease in lysosomal pH that impairs lysosomal and autophagic digestion of cellular proteins and organelles. Decreased protein degradation in XMEA may lower intracellular levels of amino acids that modulate the Mtor signaling pathway, which, in turn, upregulates macroautophagy. This leads to excessive accumulation of autophagosomes, autolysosomes, and autophagic vacuoles and a muscle-specific disease phenotype.

Female carriers are unaffected, likely because muscle is a syncytium and half of the nuclei will produce normal amounts of VMA21 mRNA. To our knowledge, XMEA is the first disease in which total, not local, cellular V-ATPase activity is affected.

On the other hand, XMEA mutations do not completely eliminate V-ATPase activity. XMEA patients do not exhibit neurodevelopmental delay or clinically manifest skin and bone abnormalities, acidosis, or hearing loss, indicating that for the specialized $\alpha 2$ -, $\alpha 3$ -, and $\alpha 4$ -containing V-ATPases the reduced V-ATPase assembly in XMEA does not reach a clinical threshold. The reduced V-ATPase activity in XMEA results in a rise in lysosomal pH from 4.7 to 5.2.

They also observed that partial inhibition of lysosomal hydrolases by leupeptin (a pH-independent inhibitor of lysosomal hydrolases) in control fibroblasts and lymphoblasts resulted in mTOR-mediated upregulation of microautophagy, reflected by proliferation of autolysosomes and autophagic vacuoles.

If the authors' notion that macroautophagy in XMEA is enhanced by activation of mTOR is correct, then blocking this pathway to reduce autophagy may prove beneficial to patients.

3.6 Features of C57 mouse

C57BL/6, often referred to as "C57 black 6" or just "black 6" (standard abbreviation: B6) is a common inbred strain of laboratory mice (fig.9).

Mice of the major C57BL substrains are black (nonagouti). The most common substrains are C57BL/6 and C57BL/10. They are named for their origin from black offspring of female number 57 to male number 52 of Miss Abby Lathrop's stock in the original mating by Clarence Cook Little in 1921. The same cross gave rise to strains C57L and C57BR. Female 58 mated with the same male gave rise to strain C58. Strains 6 and 10 separated prior to 1937. In 1946, to the Jackson Laboratory, Bar Harbor. It is probably the most widely used "genetic background" for genetically modified mice for use as models of human disease. Are often used as the host, recipient or background strain for generation of congenics carrying spontaneous or induced mutations.

They are the most widely used mouse strain, due to the availability of congeneric strains, easy breeding, and robustness. C57BL/6 mice have a dark brown, nearly black coat, and an easily irritable temperament. They have a tendency to bite, and cannot be handled like a typical pet mouse or more docile laboratory strains such as BALB/c. C57BL/6 mice have been considered to be refractory to many tumors and are used in a wide variety of research areas including cardiovascular biology, developmental biology, diabetes and obesity, osteoporosis, genetics, immunology and neurobiology research. C57BL/6 mice have a long lifespan in conventional or specific pathogen-free conditions with mean life-spans of 730 to 895 day in females and 763 to 888 days in males (22). These mice have a long live-span and presents spontaneous lesions such as: Primary lung tumors 1% in males, 3% in breeding females and zero in virgin females.

Lymphatic leukaemia is less than 2%, mammary and adenocarcinomas less than 1%(23). Leukaemia 7% (24). Rare "lipomatous" hamartomas or choristomas have been noted (25). Susceptible to the development of atheromatous lesions on wall of aorta after 20 weeks on a high-fat diet(26). Develop fatty streak-like lesions in the valve sinus region of the ascending aorta after 10-20 weeks on a diet enriched in saturated fat and cholesterol. Exhibit aortic cartilaginous metaplasia (contrast C3H) (27).

Develops noninsulin-dependent diabetes mellitus and hypertension when fed a high fat-high simple carbohydrate diet, whereas A/J mice do not (28). Susceptible to the development of atherosclerosis on a semi-synthetic high fat diet (29).

Blood glucose levels and insulin sensitivity in crosses between diet induced type II diabetes sensitive C57BL/6 and resistant A/J are genetically independent (30). High simple carbohydrate diet for five months induced hyperglycaemia, hyperinsulinaemia and hypercholesterolaemia and non-insulin-dependent diabetes mellitus which appeared to be associated with the metabolic characteristics of visceral fat (31). Gain more weight on high fat diets without consuming more calories than A/J mice and develop adipocyte hyperplasia. However, animals fed a low fat, high sucrose diet were leaner than those fed a high-complex carbohydrate diet.

These results suggest that genetic differences in metabolic response to fat are more important in the development of obesity and diabetes than caloric intake (30).

Loci on chromosomes 1, 3, 5 and 11 are associated with variation in high density lipoprotein levels with coordinate expression of cholesterol-7-alpha hydroxylase in a cross involving atherosclerosis resistant C3H/HeJ mice (32). Congenital abnormalities 10%, including eye defects, polydactyly and otocephaly (33). Microphthalmia and anophthalmia 8-20% and hydrocephalus 1-3% (34). Develop

spontaneous auditory degeneration with onset during young adulthood, with enhanced susceptibility to acoustic injury and delayed effects of toluene (contrast CBA/Ca) (35).

This is associated with early hair cell changes including bent and fused stereocilia, bulging of the cuticle plates, hair cell loss and swelling of affected dendrites (36).

C57BL/6 mice carry a single recessive gene different from that found in BALB/cBy and WB/ReJ, causing age-related hearing loss (37). Hearing loss is caused by degeneration of the organ of Corti, originating in the basal, high frequency region and then proceeding apically over time. This results in a severe sensorineural hearing loss by 14 months of age. More susceptible to noise-induced hearing loss than CBA/J (38).



FIG.9: C57 mouse phenotype

EXPERIMENTAL PART

4. Materials and Methods

For our studies we used 50 crosses of strain C57/BL6 mice, 35 male and 15 female, of different ages. The mice were sacrificed by cervical dislocation, and all organs and tissues were macroscopically and microscopically examined. we took also muscle samples from triceps muscles, quadriceps femoris, cranial tibial muscle and heart.

4.1 Light microscopy

Several sections were cut from muscle samples (10 µm thick) using the cryostat. The sections were stained with hematoxylin-eosin and Engel trichrome to focus on morphological structure and with histoenzimatic methods such as NADH, SDH, COX, ATP-ase, esterase and histochemical stains such as:

- Periodic Acid Schiff (P.A.S) to highlight the presence of mucopolysaccharides,
- Congo-Red and Crystal Violet for the presence of beta amyloid,
- Oil Red-O to highlight the presence of lipids,
- Alizarin Red to show calcium deposits.

4.2 Immunohistochemistry

Immunohistochemistry was performed on serial transverse cryostat sections (5 μm thick) of muscle specimens. Immunohistochemical detection of various antigens was performed with avidin–biotin peroxidase complex. We used antibodies against: Dystrophin rod domain (clone Dy4/6D3, Novocastra Laboratories Ltd UK, dilution 1: 50), Dystrophin c-terminus domain (clone Dy8/6C5, Novocastra Laboratories Ltd UK, dilution 1: 50), β -Sarcoglycan (clone, β Sarc/5B1, Novocastra Laboratories Ltd UK, dilution 1: 100) , γ -sarcoglycan (clone 35DAG/21B5, Novocastra Laboratories Ltd UK, dilution 1: 100) , β -Dystroglycan (clone 43DAG1/8D5, Novocastra Laboratories Ltd UK, dilution 1: 100), spectrin(clone RBC2/3D5, Novocastra Laboratories Ltd UK,dilution 1:50), Alpha2 Laminin (mouse monoclonal antibody Clone 5H2 MILLIPORE CA 92590 USA 1:200) aimed at highlighting proteins and membrane glycoproteins; Beclin-1 (BECN 1 (H300): sc-11427, Santa Cruz Biotechnology, INC, rabbit polyclonal, dilution 1: 300), LC3 (LC3B antibody (ab51520), Abcam, rabbit polyclonal, dilution 1: 3000), p62 (SQSTM- D3: sc-28359 Santa Cruz Biotechnology, INC, mouse monoclonal, dilution 1: 200), LAMP2 (ab37024 Abcam rabbit polyclonal, dilution 1: 100) for highlight the lysosomal membranes, Major Histocompatibility Complex class I (H58A mouse monoclonal antibody VMRD WA 99163 USA dilution 1: 200) and Major Histocompatibility Complex class II (TH14B mouse monoclonal antibody VMRD WA 99163 USA dilution 1: 200), C5b-9 (SC5b-9 complex Ab55811, Abcam rabbit polyclonal, dilution 1:1000).

4.3 Electron microscopy

Muscle specimens were fixed in glutaraldehyde 2,5 pH for 4 hours, then washed several times during the day at 4 °C with phosphate buffer pH 7,4 and then, the samples were postfixed in 2% osmium tetroxide for 1,30 h. Then, several treatments with ethyl alcohol at different concentrations were made, to dehydrate the samples. We left the samples in absolute alcohol overnight.

The next day, the samples were treated with a mix of resin and absolute alcohol and then, these were embedded in agar resin. Ultra-thin sections were stained with and examined with an electron microscope.

4.4 Immunoblot

From muscle samples, cryostat sections (10 µm thick) were cut, collected in a 1,5 ml tube, homogenized in RIPA lysis buffer containing 50 mM HEPES pH 7.5, 150 mM sodium chloride (NaCl), 0.25% sodium deoxycholate, 1% Triton, 1 mM ethylenediaminetetraacetic acid (EDTA). At the time of the use we added: 20 mM sodium pyrophosphate ($\text{Na}_4\text{P}_2\text{O}_7$), 0.1 mg/ml aprotinin, 2 mM phenylmethylsulfonyl fluoride (PMSF), 10 mM sodium orthovanadate (Na_2VO_3), and 50 mM sodium fluoride (NaF) (Sigma-Aldrich, Milan, Italy) by dispenser VDI 25 (VWR, Milan, Italy). Lysates were clarified by centrifugation at 11,000 g for 30 minutes. Supernatants were collected and protein concentration was measured using the Bradford assay (Bio-Rad Laboratories, Milan, Italy). For Western blotting, 50 µg of lysate proteins were heated at 100°C in 4X pre-mixed Laemmli sample buffer. Proteins were subjected to sodium dodecyl sulfate–polyacrylamide gel electrophoresis (SDS–PAGE) (7.5% and 15%

polyacrylamide) under reducing conditions. After electrophoresis, proteins were transferred on nitrocellulose filter membranes (GE Healthcare Life Sciences, Chalfont St Giles, UK) for 1h at 10 V in 192 mM glycine/25 mM Tris-HCl (pH 7.5), 10% methanol using a Trans-Blot SD Semy Dry cell (Bio-Rad Laboratories, Milan, Italy) according to the manufacturer's instructions.

Blocking of non-specific binding is achieved by placing the membrane in 5% nonfat dry milk in Tris-buffered saline (TBS, pH 7.5) for 1 h at room temperature, washed with TBS-0.1% Tween. Then, filter was probed with LC3(Novus Biologicals, Milan, Italy) and BECN1(Novus Biologicals, Milan, Italy) antibody for an overnight incubation at 4°C. After three washes in Tris-buffered saline, membrane was then incubated with horseradish peroxidase-conjugated anti-rabbit IgG (Bio-Rad Laboratories, Milan, Italy) for 1 h at room temperature. After appropriate washing steps, bound antibody was visualized by enhanced chemiluminescence system (Western Blotting Luminol Reagent, Santa Cruz Biotechnology, CA, USA).

4.5 Genetics

Genomic DNA was extracted from frozen muscle tissues using standard protocols. Briefly frozen tissue samples were homogenized with Tissue Lyser (Qiagen, Hilden, Germany) in TRIZOL solution and DNA was isolated by ethanol precipitation. The coding regions and intron-exon boundaries of the three exons were amplified by PCR. PCR was performed with AmpliTaq Gold with GeneAmp (Applied Biosystems, Foster City, CA). The reaction conditions were the followed: 10 min at 94 °C for Taq Gold activation, 35 cycles at 94 °C for 30 s, annealing at 62 °C for 30 s, extension at 72°C for 60 s, and then 5 min at 72 °C. The PCR products were purified using

QIAquick PCR Purification Kit according to the manufacturer's instructions (Qiagen). Sequencing was performed with ABI 3100 sequencer at the DNA Core Facility of the University "Magna Graecia" and by Magabace 1000 at the GECO Laboratory of IRGS "G Salvatore".

5.Result

5.1 Light microscopy

The sections stained with hematoxylin-eosin(fig.10), shows marked increase in fiber size variation, with many atrophic and some slightly hypertrophic fibers. The most prominent feature was presence of large vacuoles, both in the intermyofibrillar network and in contact with the sarcolemma. The vacuoles contained basophilic material that stained blue at hematoxylin-eosin or, in same case, optically clear. These vacuoles were seen both in the intermyofibrillar network and in contact with myofiber surface membranes. In sections stained with Engel's trichrome(fig.11), the vacuoles contained red or purple material.

Mosaic pattern of fiber type distribution revealed no selective fiber type atrophy or selectivity for vacuolar changes. The myofibrillar architecture in non vacuolated regions was normal; some focal densities with NADH-TR(fig.12) probably corresponded to reticulum modifications. The myofibrillar architecture in non-vacuolated regions is not affected. In SDH(fig.13) and COX(fig.14) stains we observed several areas of loss of activities giving to the fibers a moth-eaten aspect. In all biopsies examined, there was no fiber necrosis, no inflammatory infiltrates, no increased connective or adipose tissue proliferation. Furthermore, in all cases examined, we

observed no involvement of the heart muscle. Histochemical stains have ruled out that the vacuoles could be accumulation of amyloid or other substances such as lipids. The muscle fiber lipid and glycogen amount was normal. There was no autofluorescent pigment in the vacuoles. Some negative features were remarkable. These vacuoles were PAS negative. Calcium deposition was observed in several vacuoles. They occur as irregular deposition along the surface and were demonstrated by alizarin red. Alizarin S staining revealed calcium accumulations subsarcolemmally and inside vacuoles, as well as on the surface of some non-vacuolated fibers. Acid phosphatase activity (fig.15), indicative of lysosomes activities, was increased in the larger vacuoles but absent in the smaller ones. However, no inflammatory infiltrate was present in our muscle samples, suggesting that immune inflammatory response is also blocked by the disease, with relevance for inflammatory muscle diseases such as polymyositis and inclusion body myositis.

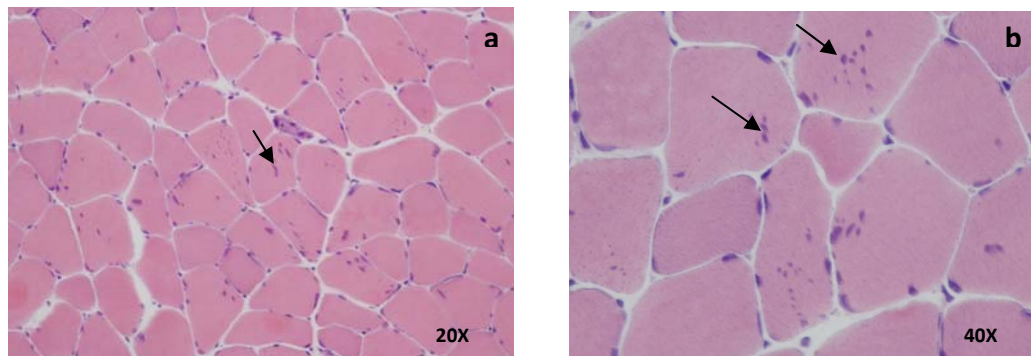


Fig.10 (a and b): *Cross-section of XMEA skeletal muscle. The vacuoles contained basophilic material that stained blue at hematoxylin-eosin (arrows).*

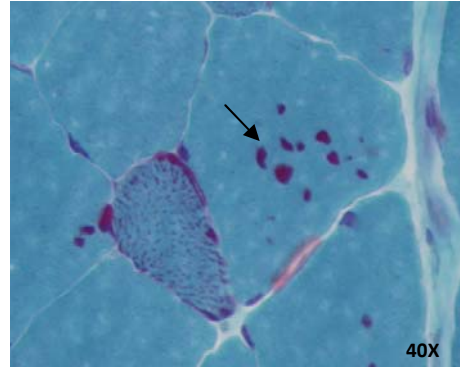
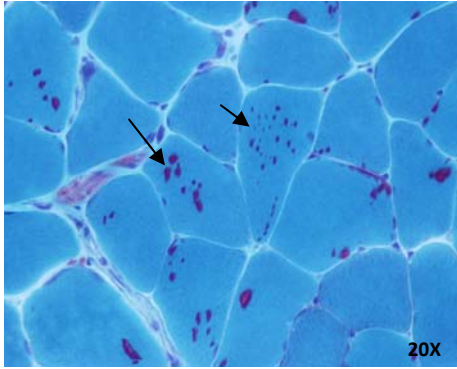


Fig.11: *In sections stained with Gomori's trichrome, the vacuoles contained red or purple material(arrows).*

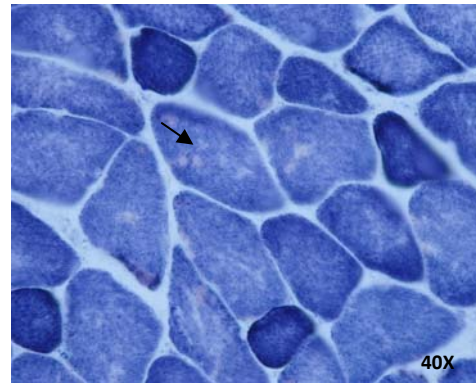
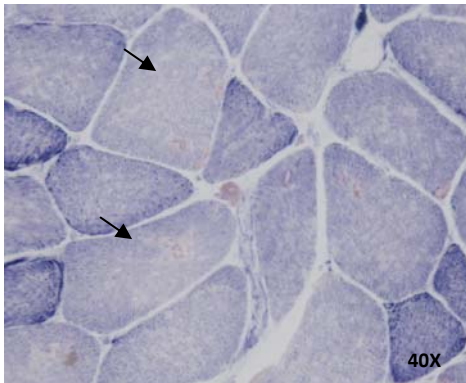


Fig.12: *NADH, areas of loss of activities corresponding to vacuoles (arrows).*

Fig.13: *SDH, several areas of loss of activities giving to the fibers a moth-eaten aspect (arrows).*

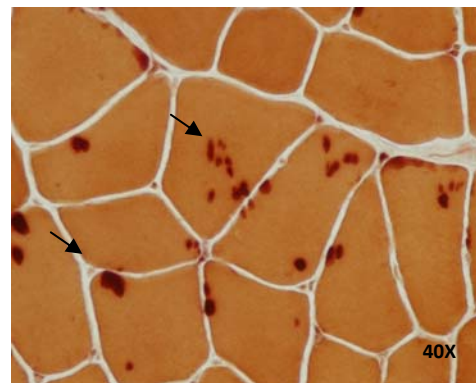
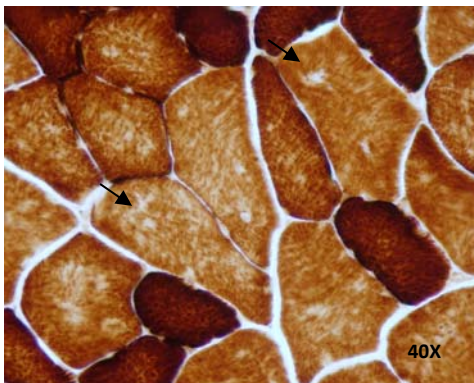


Fig.14: *COX, several areas of loss of activities giving to the fibers a moth-eaten aspect (arrows).*

Fig.15: *Esterase stain, Vacuoles Stain for Esterase (arrows).*

5.2 Immunohistochemistry

Immunohistochemical findings were the same in several cases of XMEA. In addition to the sarcolemma, numerous vacuoles and the sarcolemmal membrane lining the splitting fibers were strongly immunoreactive with antibodies directed against β spectrin, β dystroglycan, dystrophin (ROD domain, COOH domain) (fig.16), and sarcoglycans but only some were immunoreactive with anti-merosin antibody. As in normal controls, nuclei were strongly immunoreactive with anti-emerin antibody.

Some vacuoles were positive for the LAMP-2 lysosomal membrane protein (fig.17). While some vacuoles appeared positive for LC3, Beclina1 and P62.

Immunostaining with complement membrane attack complex (C5b9) antibody was positive in pathological muscle, stained strongly the vacuoles and in some fibers the sarcolemma. Anti-Major Histocompatibility Class I antigen (MHC-I) (fig.18) and Class II antigen (MHC-II) (fig.19) immunoreactivity was diffuse throughout the cytoplasm and sarcolemma of abnormal fibers and in some vacuoles. Normally, skeletal muscle does not express detectable amounts of MHC-I or MHC-II.

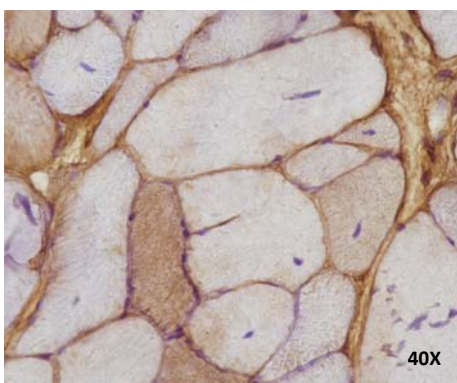


Fig.16: *Anti-COOH (dystrophin) immunostaining. Vacuoles stain for Dystrophin*

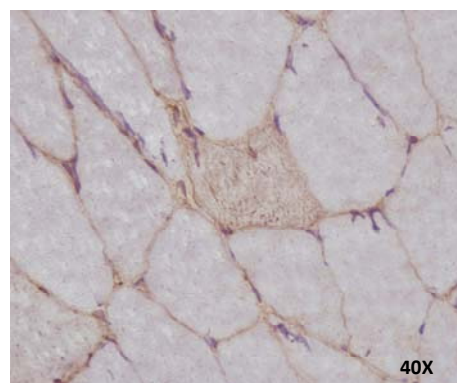


Fig.17: *Anti-LAMP-2 lysosomal membrane protein immunostaining. Brown spots represent LAMP- 2 positive signals.*

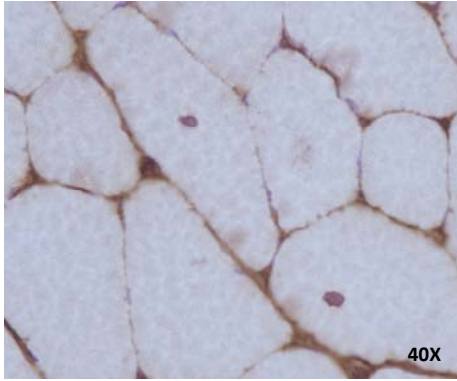


Fig.18: *Anti-MHC-I immunostaining. MHC-I signals on sarcolemma of abnormal fibers and in some vacuoles*

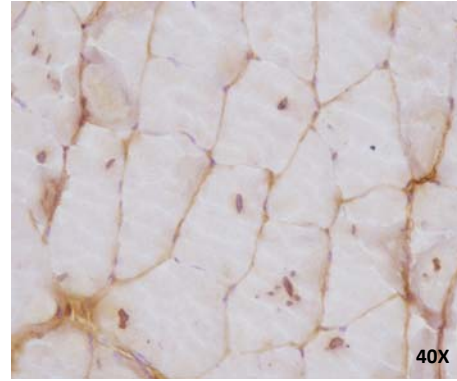


Fig.19: *Anti-MHC-II immunostaining. Black areas represent MHC-II signals on sarcolemma of abnormal fibers and in some vacuoles*

5.3 Electron microscopy

At the ultrastructural investigation, the vacuoles shows a distinctive feature from Danon disease and other AVMS: duplication of basal lamina that surrounds the abnormal muscle fibers. Vacuoles are membrane-bound and contain heterogeneous material consisting in small round dense bodies, granular material, membrane whorls, degenerative mitochondria. Smaller vacuoles are present inside the myofibers, between myofibrils, while larger ones are seen under the sarcolemma, where they seem to open and extrude their content to the extracellular space; this notion is supported by the presence of vacuolar debris and lysosomal enzymes extracellularly between the multiple layers of duplicated basal lamina.

Ultrastructural features were similar in all cases. This material was seen between infolded sarcolemma and the redundant layers of basement membrane. These formations occupied a large portion of the muscle fiber surface. The subsarcolemmal vacuoles corresponded to two different types: (1) vacuoles delimited by a dual

membrane with the inner membrane composed of basal lamina, and (2) autophagic vacuoles bounded only by a membrane. The deep sarcoplasmic vacuoles also corresponded to both types. The first type resulted from sarcolemmal invaginations and fiber splitting. The second type resulted from autophagy, because numerous electron dense bodies were not bounded by a membrane and were associated with T system proliferation. Increased triads were observed. There was no myofibrillar changes, no mitochondrial abnormalities, and no lipid storage.

In female carriers, only few muscle fibers contain autophagic vacuoles; no accumulation of lysosomal enzymes was seen intracytoplasmic or around sarcolemma.

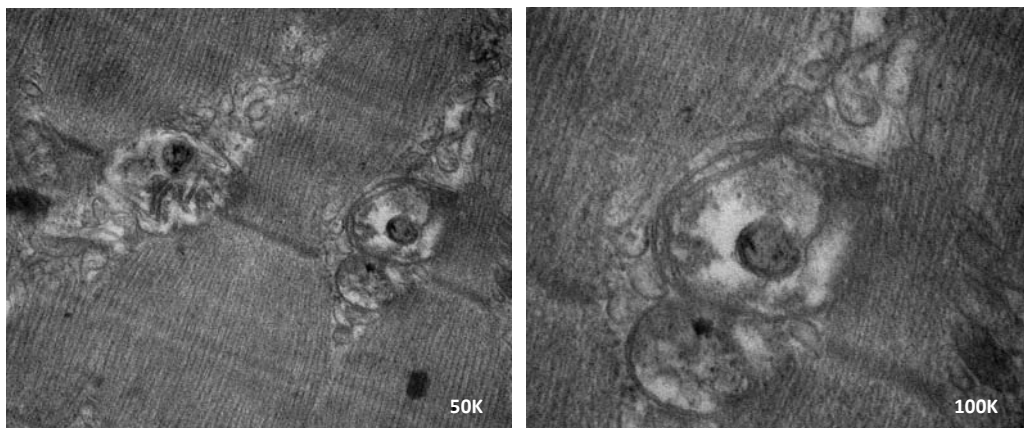


Fig.20 Electron microscopy in XMEA, electron micrographs of skeletal muscle biopsies from mouse showing autophagic vacuoles; Magnification 50k. 100k.

5.4 Immunoblot

For western blotting analyses, we used antibodies against Beclin1, P62, and LC3 surveys in order to test the markers of autophagy.

We found bands at 60 kDa, 65 kDa and 15 kDa, corresponding to Beclin, P62 and LC3 respectively.

5.5 Genetics

VMA21 protein sequence, of 101 amino acid residues, is highly conserved between human and mouse, as showed in figure 21. In order to identify if the hypomorphic mutations founded in human VMA21 gene by Ramachandran et al. (11) are also present in the mice showing the skeletal muscle disorder we analyzed the complete sequence of murine VMA21 gene. It is located on chromosome X, with three exons and transcript length of 4195 base pairs (fig. 22, panel a). We made a sequence alignment between the human and mouse gene to allow the homology identification in the six single-nucleotide carrying the substitutions described for the XMEA patients.

We used the ClustalW2 multiple sequence alignment program for DNA (www.ebi.ac.uk/Tools/msa/clustalw2/). The gene alignments are showed in figure 22, panel b. In particular we reported the sequence of the intron-exon junctions for exon 2 and 3 involved in mRNA splicing efficiency, and the initial sequence of 3'UTR, involved in the mRNA stability. We founded two conserved nucleotide, highlighting the with the four nucleotide positions described by Ramachandran et al. (11) mutated in human gene sequence of XMEA patients. There are ongoing sequence analysis on all three exons and the flanking intronic regions conducted on DNA extracted from affected mice and control animals to determine whether a significant association existed between the pathologic phenotype and the gene expression of VMA21.

```

Homo      MERPDKAALNALQPPEFRNESSLASTLKTLLFFFTALMITVPIGLYFTTKSYIFEGALGMS 60
Mus       MERLDKAALNALQPPEFRNENSLAATLKTLLFFFTALMITVPIGLYFTTKAYIFEGALGMS 60
          *** *****.***;*****;*****
Homo      NRDSYFYAAIVAVVAVHVVLALFVYVAWNEGSRQWREGKQD 101
Mus       NRDSYFYAAIVAVVAVHVVLALFVYVAWNEGSRQWREGKQD 101
          *****
    
```

Fig.21 VMA21 mouse gene: *Human and mouse protein sequence alignment*

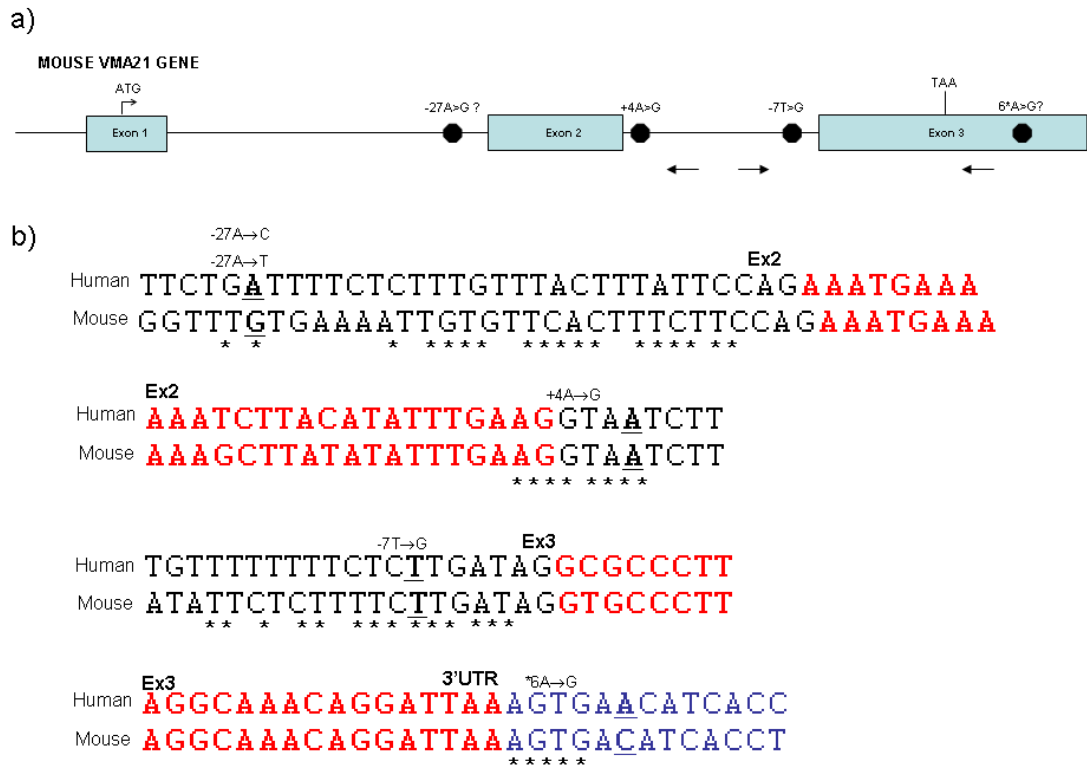


Fig.22 VMA21 mouse gene

(A) Schematic diagram of VMA21 mouse gene, with the exons (rectangles). The positions of the human corresponding mutations are indicated by bullets. The PCR primer positions are indicated by arrows (B) Human and mouse gene alignment in the intron-exon junctions for exon 2, 3 indicated in red and black, respectively, and the 3'UTR indicated in blue. The human corresponding positions of mutations are underlined.

6. Discussion

In this thesis, we described a spontaneous mouse model of XMEA a diseases, first reported in 1988 by Kalimo et al.(15) in a Finnish family, and then in a French family by Villanova et al.(39).

Genetic analysis in Kalimo's family suggested a linkage to Xq-28, although the lod score was not significant.

Multipoint linkage analysis confirmed the assignment of this locus with a maximal lod score of 2.74 obtained at recombination fraction zero. This was further confirmed recently by Auranen et al.(19) Moreover these authors assign the XMEA gene locus to the most telomeric 10.5 cM of chromosome X. It was demonstrated that the gene responsible for XMEA is a chaperone for the assembly of the organellar acidification pump, the vacuolar ATPase. This explains decreased acidification in lysosomes throughout muscle having as a late result the formation of autophagic vacuoles. The main chaperone directing assembly of the V0 integral membrane domain of the VATPase pump is the Vma21 protein. It was demonstrated that *vma21* deletion mutant (*vma21*Δ) has drastically reduced V-ATPases and VATPase activity in organellar membranes and cause X-linked myopathy with excessive autophagy.

XMEA mutations are hypomorphic alleles that reduce the amount of VMA21, in most cases by decreasing mRNA splicing efficiency. Only skeletal muscle is clinically affected, and only in males. Female carriers are unaffected, likely because muscle is a syncytium and half of the nuclei will produce normal amounts of VMA21 mRNA.

We analyzed the complete sequence of murine VMA21 gene and found that VMA21 protein sequence, of 101 aminoacid residues, is highly conserved between

human and mouse. We made a sequence alignment between the human and mouse gene to allow the homology identification in the the six single-nucleotide carrying the substitutions described for the XMEA patients and we found some differences but there are ongoing sequence analysis to determine whether a significant association existed between the pathologic phenotype and the gene expression regulation of VMA21.

Clinically, it is difficult to define the age of disease onset due to a paucity of early clinical symptoms. Otherwise, childhood onset was most common. The course of the disease was very slow; the clinical condition remained static during the 5 years of observation. Moderate proximal weakness, most prominent in the lower limbs was noted in most cases. In some patients, muscle weakness was also present in upper limb girdle muscles. There was no cardiac involvement. Among the patients reported in the literature, five died but the death was not myopathy related. Thus, longevity is not altered in most cases of XMEA. In all cases, the serum CK concentration was clearly elevated and usually before the onset of clinical symptoms.

Morphological features were identical in all muscle samples, but the pathogenesis of the vacuole formation as well as their content remain unknown. Muscle specimens showed numerous vacuoles in subsarcolemmal spaces and in the intermyofibrillar network. Necrotic and regenerative fibers were absent. We demonstrated a marked deposition of the complement membrane attack complex C5b-9 on the damaged cell surface membrane suggesting that these deposits could be important in the pathogenesis of this myopathy and that the membrane bound vacuoles might be the consequence of sarcolemma invagination, as confirmed also with the positivity of dystrophin proteins on the vacuoles membrane. In addition, we demonstrated calcium accumulation on sarcolemma, which is likely secondary to the membrane attack complex deposition on the cell surface.

By EM, besides the evident features of autophagic vacuoles, we and other authors, observed that subsarcolemmal and intermyofibrillar vacuoles are bounded both by basement and sarcolemmal membranes. Moreover, immunohistochemistry showed that the vacuolar membranes were immunoreactive with β spectrin, dystrophin, sarcoglycan, and merosin. Furthermore, the invaginating sarcolemmal membrane also showed similar immunoreactivities.

In contrast, vacuolar membranes in lysosomal glycogen storage diseases did not express dystrophin, sarcoglycan, and merosin, although both dystrophin and β spectrin were previously immunolocalized to vacuolar membranes in these diseases.

These results strongly suggest that both autophagic activity and sarcolemmal invagination occurs in our cases such as in XMEA.

As previously reported, we also observed anti-C5b-9 immunoreactivity and calcium deposits on the cytoplasmic membrane of all vacuolated fibers and in some non-vacuolated fibers. Interestingly C5b-9 deposits were also present within some vacuoles. Thus the abnormal material accumulated within the vacuoles in XMEA corresponds to both calcium and C5b-9 deposits. It was previously suggested that 'calcium accumulation on sarcolemma is secondary to C5b-9 deposition on the cell surface and could probably correspond to the calcium entering through C5b-9 channels. This hypothesis however should be modulated. First, not all calcium positive fibers were MAC positive, suggesting that calcium accumulation may precede MAC accumulation. Second, abnormal MAC deposition may occur without calcium deposition in a large number of non-necrotic muscle fibers in numerous muscular dystrophies. In our opinion, the cell surface membrane deposition of calcium and its abnormal accumulation within the vacuoles are the most salient features of this myopathy.

It was suggested that the primary event in XMEA is an unknown membranous

alteration likely affecting both plasma and T-tubule membranes leading to calcium deposition and MAC accumulation with subsequent membranous invagination. Moreover the T-tubule membrane may be involved in the formation of the autophagic vacuoles observed in XMEA(41).

Endocytosis of the MAC -positive membranes may protect the muscle fibers against the lytic action of the MAC. Class I and II MHC antigen were also expressed on the periphery of vacuoles but their expressions were not related to inflammatory changes. In summary, XMEA exhibits features not seen in any other muscle disease: persistent MAC on and calcium accumulation in non-necrotic myofibers, and expression of MHC class I and II antigens in the absence of any inflammation. Myofiber demise appears to occur through a novel form of autophagic cell death.

Giant autophagic vacuoles encircle sections of cytoplasm including organelles, proteins, glycogen, calcium-containing compartments and membrane whorls. The vacuoles contain lysosomal hydrolases, yet appear unable to complete digestion of their contents. Instead, they migrate to the myofiber surface, fuse with the sarcolemma, and extrude the contents extracellularly, forming a field of cell debris rich in lysosomal enzymes around the fiber.

On the other hand, XMEA mutations do not completely eliminate V-ATPase activity. XMEA patients do not exhibit neuro-developmental delay or clinically manifest skin and bone abnormalities, acidosis, or hearing loss, indicating that for the specialized $\alpha 2$, $\alpha 3$ and $\alpha 4$ -containing V-ATPases the reduced V-ATPase assembly in XMEA does not reach a clinical threshold.

The literature also substantiates that decreased V-ATPase causes the autophagic block through raising lysosomal pH, and not through some alternate mechanism.

XMEA is a vacuolar myopathy with a unique pathology. Understanding mechanisms

underlying this particular type of vacuolation and its relationship with autophagy progression, autophagic cell death, necrosis and inflammation is of great interest for future therapies not only of XMEA, but also a large number of diseases where these processes are affected.

Although the lesions of XMEA are not entirely specific, the observations reported in the mouse model that we studied, are similar to those described in the literature so far. It remains to be investigated whether this disease is caused by a mutation of a protein membrane-associated lysosomal sarcolemmal of a protein or a protein common to both membrane systems.

In conclusion, the unique pathological features observed in XMEA are characteristic and suggest a new pathophysiological mechanism.

Understanding the pathogenesis of this unusual type of vacuolation would not only help solve autophagic vacuolar myopathies and initiate appropriate therapies, but also give insights toward the autophagic process and its deregulation in disease.

Autophagy is a process whose molecular characterization is recent and on-going. It is relevant for a large variety of human diseases, from infections to neurodegenerative disorders and to cancers.

The availability of a well characterized mouse model, as we are proposing, it may help to define the etiopathogenesis of this disease and the VMA21 mutation may reveal the reasons for the muscle specific phenotype of XMEA.

7. References

1. Nishino, I., "Autophagic vacuolar myopathies". *Curr Neurol Neurosci Rep*, 2003. 3(1): p.64-9.
2. Fukuda, T., K. Zaal, E. Ralston, P.H. Plotz, and N. Raben, "Dysfunction of endocytic and autophagic pathways in a lysosomal storage disease". *Ann Neurol*. 2006 Apr;59(4):700-8.
3. Nishino, I., J. Fu, K. Tanji, T. Yamada, S. Shimojo, T. Koori, M. Mora, J.E. Riggs, S.J. Oh, Y. Koga, C.M. Sue, A. Yamamoto, N. Murakami, S. Shanske, E. Byrne, E. Bonilla, I. Nonaka, S. DiMauro, and M. Hirano, "Primary LAMP-2 deficiency causes X-linked vacuolar cardiomyopathy and myopathy (Danon disease)". *Nature*, 2000. 406(6798): p.906
4. Tanaka, Y., G. Guhde, A. Suter, E.L. Eskelinen, D. Hartmann, R. Lullmann-Rauch, P.M. Janssen, J. Blanz, K. von Figura, and P. Saftig, "Accumulation of autophagic vacuoles and cardiomyopathy in LAMP-2-deficient mice". *Nature*, 2000. 406(6798): p. 902-6.
5. Saftig, P., W. Beertsen, and E.L. Eskelinen, "LAMP-2: a control step for phagosome and autophagosome maturation". *Autophagy*, 2008. 4(4): p. 510-2.
6. "Myology" Andrew G. Engel, Clara Franzini-Armstrong. Chapter 28 "Lysosomal Metabolism and its relevance to skeletal muscle. P.708-733
7. Yamamoto A, Morisawa Y, Verloes A, Murakami N, Hirano M, Nonaka I, Nishino I. "Infantile autophagic vacuolar myopathy is distinct from Danon disease" *Neurology*. 2001 Sep 11;57(5):903-5.

8. Yan C, Tanaka M, Sugie K, Nobutoki T, Woo M, Murase N, Higuchi Y, Noguchi S, Nonaka I, Hayashi YK, Nishino I." A new congenital form of X-linked autophagic vacuolar myopathy" *Neurology*. 2005 Oct 11;65(7):1132-4.
9. Kaneda D, Sugie K, Yamamoto A, Matsumoto H, Kato T, Nonaka I, Nishino I." A novel form of autophagic vacuolar myopathy with late-onset and multiorgan involvement" *Neurology*. 2003 Jul 8;61(1):128-31.
10. Sugimoto S." A novel vacuolar myopathy with dilated cardiomyopathy." *Autophagy*. 2007 Nov-Dec;3(6):638-9. Epub 2007 Aug 23.
11. Ramachandran N, Munteanu I, Wang P, Aubourg P, Rilstone JJ, Israelian N, Naranian T, Paroutis P, Guo R, Ren ZP, Nishino I, Chabrol B, Pellissier JF, Minetti C, Udd B, Fardeau M, Tailor CS, Mahuran DJ, Kissel JT, Kalimo H, Levy N, Manolson MF, Ackerley CA, Minassian BA." VMA21 deficiency causes an autophagic myopathy by compromising V-ATPase activity and lysosomal acidification." *Cell*. 2009 Apr 17;137(2):235-46.
12. Xie Z, Klionsky DJ." Autophagosome formation: core machinery and adaptations" *Nat Cell Biol*. 2007 Oct;9(10):1102-9.
13. Bechet, D., A. Tassa, D. Taillandier, L. Combaret, and D. Attaix, "Lysosomal proteolysis in skeletal muscle". *Int J Biochem Cell Biol*, 2005. 37(10): p. 2098-114.
14. Mizushima, N., A. Yamamoto, M. Matsui, T. Yoshimori, and Y. Ohsumi," In vivo analysis of autophagy in response to nutrient starvation using transgenic mice expressing a fluorescent autophagosome marker". *Mol Biol Cell*, 2004. 15(3): p. 1101-11.
15. Kalimo, H., M.L. Savontaus, H. Lang, L. Paljarvi, V. Sonninen, P.B. Dean, K.

Katevuo, and A. Salminen,” X-linked myopathy with excessive autophagy: a new hereditary muscle disease”. *Ann Neurol*, 1988. 23(3): p. 25

16. Jaaskelainen, S.K., V.C. Juel, B. Udd, M. Villanova, R. Liguori, B.A. Minassian, B.Falck, P. Niemi, and H. Kalimo,” Electrophysiological findings in X-linked myopathy with excessive autophagy”. *Ann Neurol*, 2002. 51(5): p. 648-52.

17. Saviranta P, Lindlöf M, Lehesjoki AE, Kalimo H, Lang H, Sonninen V, Savontaus ML, de la Chapelle A. “Linkage studies in a new X-linked myopathy, suggesting exclusion of DMD locus and tentative assignment to distal Xq.” *Am J Hum Genet*. 1988 Jan;42(1):84-8.

18. Villard L, des Portes V, Levy N, Louboutin JP, Recan D, Coquet M, Chabrol B, Figarella-Branger D, Chelly J, Pellissier JF, Fontes M.” Linkage of X-linked myopathy with excessive autophagy (XMEA) to Xq28.” *Eur J Hum Genet*. 2000 Feb;8(2):125-9.

19. Auranen, M., M. Villanova, F. Muntoni, M. Fardeau, S.W. Scherer, H. Kalino, and B.A.Minassian, X-linked vacuolar myopathies: two separate loci and refined genetic mapping. *Ann Neurol*, 2000. 47(5): p. 666-9.

20. Forgac M.” Vacuolar ATPases: rotary proton pumps in physiology and pathophysiology.” *Nat Rev Mol Cell Biol*. 2007 Nov;8(11):917-29.

21. Hirano M, DiMauro S.” VMA21 deficiency: a case of myocyte indigestion” *Cell*. 2009 Apr 17;137(2):213-5.

22.”The Mouse in Biomedical Research” J.G.Fox, S.W.Barthold, M.T.Davisson, C.E. Newcomer, F.W. Quimby, A.L.Smith. Vol I.

23. Hoag WG. ”Spontaneous cancer in mice” *Ann N Y Acad Sci*. 1963 Nov 4;108:805-

31.

24. Myers DD, Meier H, Rhim JS, Huebner RJ." Excretion of murine leukaemia virus" Nature. 1970 May 30;226(5248):849-50.

25. Adkison DL, Sundberg JP." "Lipomatous" hamartomas and choristomas in inbred laboratory mice" Vet Pathol. 1991 Jul;28(4):305-12.

26. Roberts A, Thompson JS." Inbred mice and their hypbrids as an animal model for atherosclerosis research" Adv Exp Med Biol. 1976;67(00):313-327.

27. Qiao JH, Fishbein MC, Demer LL, Lusis AJ." Genetic determination of cartilaginous metaplasia in mouse aorta." Arterioscler Thromb Vasc Biol. 1995 Dec;15(12):2265-72.

28. Mills E, Kuhn CM, Feinglos MN, Surwit R." Hypertension in CB57BL/6J mouse model of non-insulin-dependent diabetes mellitus" Am J Physiol. 1993 Jan;264(1 Pt 2):R73-8.

29. Nishina PM, Wang J, Toyofuku W, Kuypers FA, Ishida BY, Paigen B." Atherosclerosis and plasma and liver lipids in nine inbred strains of mice." Lipids. 1993 Jul;28(7):599-605.

30. Surwit RS, Seldin MF, Kuhn CM, Cochrane C, Feinglos MN." Control of expression of insulin resistance and hyperglycemia by different genetic factors in diabetic C57BL/6J mice". Diabetes. 1991 Jan;40(1):82-7.

31. Rebuffé-Scrive M, Surwit R, Feinglos M, Kuhn C, Rodin J." Regional fat distribution and metabolism in a new mouse model (C57BL/6J) of non-insulin-dependent diabetes mellitus." Metabolism. 1993 Nov;42(11):1405-9.

32. Moore GL, Drevon CA, Machleder D, Trawick JD, McClelland A, Roy S, Lyons R, Jambou R, Davis RA." Expression of human cholesterol 7 α -hydroxylase in atherosclerosis-susceptible mice via adenovirus infection" *Biochem J.* 1997 Jun 15;324 (Pt 3):863-7.
33. Kalter H." Sporadic congenital malformations of newborn inbred mice" *Teratology.* 1968 May;1(2):193-9.
34. Dagg CP, Schlager G, Doerr A." Polygenic control of the teratogenicity of 5-fluorouracil in mice". *Genetics.* 1966 Jun;53(6):1101-17.
35. Li HS, Borg E." Auditory degeneration after acoustic trauma in two genotypes of mice." *Hear Res.* 1993 Jun;68(1):19-27.
36. Hultcrantz M, Li HS." Inner ear morphology in CBA/Ca and C57BL/6J mice in relationship to noise, age and phenotype" *Eur Arch Otorhinolaryngol.* 1993;250(5):257-64
37. Willott JF, Erway LC, Archer JR, Harrison DE." Genetics of age-related hearing loss in mice. II. Strain differences and effects of caloric restriction on cochlear pathology and evoked response thresholds" *Hear Res.* 1995 Aug;88(1-2):143-55.
38. Davis RR, Newlander JK, Ling X, Cortopassi GA, Krieg EF, Erway LC." Genetic basis for susceptibility to noise-induced hearing loss in mice" *Hear Res.* 2001 May;155(1-2):82-90.
39. Villanova, M., J.P. Louboutin, D. Chateau, B. Eymard, M. Sagniez, F.M. Tome, and M. Fardeau, "X-linked vacuolated myopathy: complement membrane attack complex on surface membrane of injured muscle fibers." *Ann Neurol*, 1995. 37(5): p. 637-45.
40. Louboutin, J.P., M. Villanova, B. Lucas-Heron, and M. Fardeau," X-linked

vacuolated myopathy: membrane attack complex deposition on muscle fiber membranes with calcium accumulation on sarcolemma”. *Ann Neurol*, 1997. 41(1): p. 117-20.

41. Nishino, I., “Autophagic vacuolar myopathies”. *Curr Neurol Neurosci Rep*, 2003. 3(1): p.64-9.

LIST OF INTERNET RESOURCES

-Neuromuscular Disease Center - Washington University, St. Louis, MO, USA

<http://neuromuscular.wustl.edu/index.html>

-www.ebi.ac.uk/Tools/msa/clustalw2/